Cross section for $C(\alpha,X)^{11}C$ at 0.64–2.8 GeV

J. R. Radin,[a]* H. Quechon,[b] G. M. Raisbeck,[a] and F. Yiou[a]
[a]*Laboratoire René Bernas du Centre de Spectrométrie Nucléaire et de Spectrométrie de Masse, 91406 Orsay, France*
[b]*Centre d'Etudes Nucléaires de Saclay, Service de Protection contre les Rayonnements, 91191 Gif-sur-Yvette, France*
(Received 1 September 1982)

The absolute cross section for the reaction $C(\alpha,X)^{11}C$ has been measured from 0.64 to 2.8 GeV using a counter telescope to determine the alpha flux and a plastic scintillator target to determine the ^{11}C activity. The results are 55.6 ± 2.2 mb (0.64 GeV), 49.2 ± 1.9 mb (1.2 GeV), 44.1 ± 1.8 mb (2.0 GeV), and 42.0 ± 1.7 mb (2.8 GeV).

[NUCLEAR REACTIONS $C(\alpha,X)^{11}C$, $E=0.64$, 1.2, 2.0, 2.8 GeV; measured absolute cross section.]

I. INTRODUCTION

The number of particles in the intense beams delivered by accelerators in the intermediate and high energy regions is generally measured indirectly, very often using activation reactions. One such reaction, particle + $C\rightarrow{}^{11}C+X$, is widely used and serves as a reference,[1,2] since its cross section is relatively easily determined. Because of its mode of disintegration and the fact that it can be produced in a plastic scintillator, ^{11}C induced activity can be measured by an absolute method. Even with the low intensity beams necessary when using absolute measurement techniques (scintillation counter telescope, nuclear emulsions), the induced activity can still be easily measured because of the short half-life of ^{11}C and the fairly large cross sections. While the excitation function of the proton-induced reaction $C(p,X)^{11}C$ is quite well known between 20 MeV and 300 GeV (Refs. 1–3), cross section values for reactions induced by other particles are scarcer and available only for much narrower energy ranges. Thus, when this work was begun, the excitation function of the helion induced reaction $C(\alpha,X)^{11}C$ was known only up to 380 MeV,[2] beyond which one single cross section measurement had been made at 920 MeV.[4] Using the Saclay synchrotron Saturne I, we measured the cross section of this reaction for subsequent use as a primary monitor of alpha beams delivered by accelerators between 0.1 and 1 GeV per nucleon.

II. EXPERIMENTAL PROCEDURE

As discussed by Cumming,[1] techniques available for determining absolute cross sections of high energy reactions are quite limited. In the present experiment, the alpha particle flux crossing a plastic scintillator target in association with a counter telescope was determined (Fig. 1a); the number of ^{11}C atoms was measured by means of the internal scintillation produced from the ^{11}C positron decay in the target. Once the system is in operation, a significant advantage of this method is the possibility of making multiple determinations with only a slight increase in effort. Its main drawback is the need to use low intensity, well-controlled beams. This latter restriction has been somewhat lessened by the availability of faster electronic systems, but a careful approach is still required.

A. Beam and telescope

The accelerator beam intensity was initially reduced to a minimum ($\approx10^8$ particles per cycle) compatible with stable machine operation, which requires continuous feedback of the internal beam. The beam was extracted using a resonance extraction system and it was passed through variable collimators adjusted to give the desired maximum operating flux ($\approx10^6$ particles/pulse). The beam could then be further reduced by using a steering

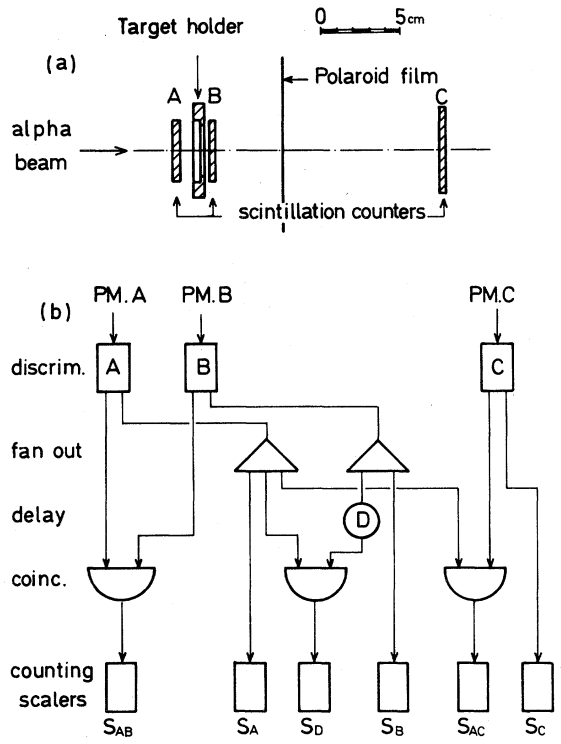

FIG. 1. Schematic diagram of the plastic scintillator telescope system (a) and its associated electronics (b).

magnet to direct only a portion of the available particles through the second part of the beam line. It was then passed through several more sets of bending and focusing magnets before arriving at the counter telescope. Possible contamination of the beam by deuterons and/or neutrons is discussed below. This beam line cannot transport the maximum energy alpha beam (4.6 GeV) of the machine, so our measurements had to be limited to 2.8 GeV.

The telescope consisted of three scintillators (NE 102 A) with the target placed between the first two scintillators, as shown in Fig. 1(a). All three were 3 mm thick; the first two (A and B) having the same diameter as the targets (38 mm). The third (C) was larger (55 mm) in order to permit checks of beam alignment and possible losses due to scattering, beam size, etc. The scintillators were connected by 8 cm light pipes to XP 2020 photomultipliers, with appropriate absorbers at the photomultiplier interface for optimum operation at $\approx$2000 V. The post-photomultiplier electronics, shown schematically in Fig. 1(b), featured 60 mV discriminator thresholds, 4 ns pulse widths, and nominal dead times of 10 ns (time-over-threshold discriminator). These characteristics were verified by a double pulse generator. However, in-beam measurement and analysis of dead time losses suggest somewhat different "effective" characteristics (see the Appendix). For each exposure, the integrated number of counts of singles (S_A, S_B, S_C) pulses, prompt coincidences (S_{AB}, S_{AC}), and delayed coincidences (S_D, with a delay of 35 ns between A and B) were recorded. The coincidence S_{AB} gives the raw measure of alpha particles, while S_D enables evaluation of dead time losses (delayed coincidences were not employed for the 0.64 GeV exposures). Every ten pulses, a running total of S_{AB} was also recorded so that variations in beam intensity during an exposure could be corrected. The time between pulses varied from 2 to 2.4 s depending on the energy of the beam. The time profile of the extracted beam was in the approximate form of a triangle with a FWHM of $\approx$100 ms. In an attempt to reduce the microstructure of the extracted beam to a minimum, the radiofrequency of the machine was turned off before extraction. Nevertheless, some structure was still evident. The exposures were made at average intensities of 2×10^4 to 4×10^5 alphas/pulse, which gave estimated instantaneous rates (deduced from the random coincidence rates) of 3×10^5 to 8×10^6 alphas/s. Exposures lasted from 5–15 min, giving total integrated fluxes of $5\times10^6-7\times10^7$ alpha particles.

B. Targets and ^{11}C counting

The targets were 3, 6, or 10 mm thick disks of NE 102 A or PILOT B scintillator plastic, 38 mm in diameter and polished on all sides. The beam spot size, checked before and during each exposure by radioautograph (Polaroid film), was normally $\leq$2 cm in diameter. In order to check possible edge or alignment effects, two exposures were made with the beam deliberately defocused so as to be much larger than the telescope diameter. The results were in excellent agreement with the normal runs, confirming an absence of problems. The ^{11}C measurements of the irradiated targets were made in an underground counting facility, where they were optically coupled with glycerol. A small light pipe attached to a 5 cm photomultiplier tube (56 DVP) served to center the scintillator and hold the optical coupling fluid. The mounting procedure was performed under red light to reduce photocathode excitation. The whole assembly was shielded by 5 cm of lead. The photomultiplier signals were processed through a standard preamplifier-amplifier-discriminator-scaler system. The discriminator level was set at 60 keV using the γ rays from an ^{241}Am

source, which was checked at each run with a multichannel pulse height analyzer. An automatic control system was used to print out and reset the counting system every two minutes, with the decay being followed from 2 to 4 ^{11}C half-lives. The time between the end of exposure and the beginning of counting was from 8 to 12 mins, and initial ^{11}C count rates were 250–3000 cpm. To increase the rate of data taking, two systems identical to that described above were used.

III. ANALYSIS OF DATA

A. ^{11}C counting

Using a least squares program, the ^{11}C decay curves were fitted to two components, one having a half-life of 20.39 min, the other a constant background, which was measured for the targets several days after irradiation, when all the ^{11}C had decayed. Fits were also made leaving the background quantity a free parameter. Averaged over all exposures, the difference in ^{11}C fits between the two procedures was (0.8 ± 0.9) %. The measured background fit was used in the final cross section calculation. The average χ^2 for these fits was 1.2 ± 0.3. The average calculated error in the ^{11}C from the decay fits is (1.0 ± 0.4) %. From the measured ^{11}C activity, the total number of ^{11}C formed was calculated by correcting for decay during irradiation, including effects of variable beam intensity. A branching ratio of 0.998 was assumed for ^{11}C β^+ decay. A carbon weight fraction of 0.9152 was used for both NE 102 and PILOT B targets. The targets were thick enough for effects due to ^{11}C diffusion losses to be neglected.[2]

^{11}C detection efficiencies have been measured in separate experiments, with higher intensity beam, by the 4π β-γ coincidence method.[5–7] Experiments were carried out with 3, 6, and 10 mm thick targets, and with 16, 50, and 60 keV energy thresholds (the discrimination threshold was calibrated in energy with ^{55}Fe, ^{57}Co, ^{65}Zn, ^{109}Cd, and ^{241}Am sources). A summary of results, together with previous measurements[5,8–11] under similar conditions, is given in Fig. 2, which is a plot of the detection efficiency variation versus scintillator thickness for all the three thresholds. In cross section calculations, efficiency values of 0.930, 0.945, and 0.955 (±0.010) were used (the β detection threshold being fixed at 60 keV) with 3, 6, and 10 mm thick targets, respectively.

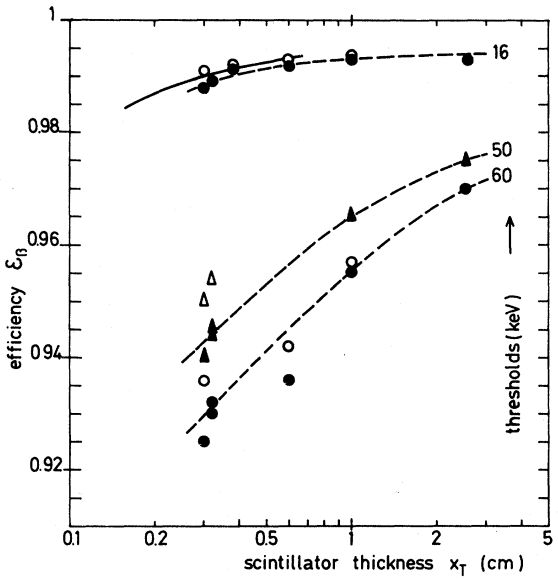

FIG. 2. ^{11}C detection efficiency ϵ_β as a function of scintillator thickness x_T for 16, 50, and 60 keV thresholds. References 8–11 for 3.2 mm thickness, Ref. 11 for 3.8 mm, Ref. 5 for 25.4 mm, and this work for 3, 6, and 10 mm (error bars are omitted for the sake of simplicity; 0.5 to 1 % for 50 and 60 keV thresholds, 0.1 to 0.2 % for 16 keV). ○, △, denote efficiency with thick reflector screen (1.5–1.6 mm Al); ●, ▲ denote efficiency with thin reflector; the triangle is for the 50 keV threshold. The solid curve is the best fit (Ref. 11) of nine results for scintillator thickness between 0.16 and 0.66 cm with a thin reflector and narrow beam ($\epsilon_\beta=0.9964-0.0019/x_T$). The dashed curves are guides for the eye, only for thin reflector.

B. Corrections

1. Effect of target on coincidence AB. A number of comparisons of the coincidences to singles ratio S_{AB}/S_A were made at 1.2 GeV, with and without target. This enabled us to establish a correction factor of 3.4×10^{-3} x_T for the measured coincidence rate, where x_T is the thickness of the target in g/cm^2. This same factor was used to correct the measured beam flux at all energies.

2. Dead time corrections. As mentioned earlier, the experimental technique adopted requires a careful evaluation of dead time effects. This is especially true in our case because of the relatively poor duty cycle of the available α beam and the resulting high instantaneous particle fluxes. The methods we considered for making these corrections are described in the Appendix. To use these methods requires making a sufficient number of exposures over a large enough range of intensities.

3. Deuteron contamination. One of the disadvantages of reducing the beam by collimation is that a significant number of ^{2}H are produced by the breakup of alphas on the collimator edges, so that any ^{2}H produced with little momentum change can be transported and focused with the alphas, and so produce ^{11}C in the target. Having the same rigidity as the alpha, these ^{2}H will give a signal in the telescope. This signal is equal to one quarter of the alpha's, a value below the setting of the telescope discriminator levels. To look for such particles, we monitored the output of one of the telescope scintillators on an oscilloscope. There was occasional evidence of them, particularly when the steering magnet reduced the beam intensity to its lowest level (in these conditions, there is a tendency to take the "tail" of the main beam, hence there is a greater susceptibility to edge effect in the collimator). We have no quantitative information on the magnitude of this ^{2}H contamination. Comparison of exposures containing this contamination with those where none was seen gives no systematic differences within our detectable limits ($\approx 3\%$), which indicates that the effect of this occasional contamination is small. We have therefore allowed for a possible 3% systematic error in our final results to cover this effect.

4. Neutron contamination. To check for the effects of fast neutron background at the position of our experiment, a "blank" target was placed ≈ 10 cm to one side of the telescope during one of our 2.8 GeV exposures. The activity of this blank was 2.6% of the irradiated target. This can probably be considered an upper limit since it neglects any contribution from a charged particle "halo" at this position. For this reason, a correction of $(-1.3\pm 1.3)\%$ has been made, which assumes the neutron contribution to be the same at the position of the telescope, and to be constant for all energies and intensities.

5. Secondary production. Many of the alphas which interact in the target give rise to high energy secondary particles, which can also produce ^{11}C. These are mostly in the forward direction, and we have estimated their effect in separate experiments by exposing target stacks in a high beam intensity and comparing the specific activity in the front and back disks. The results of these experiments lead to the coefficient of secondary activity production α (in cm^2/g), which depends on energy in the following form:

$$\alpha = 0.0665 + 0.0388 \ln E_\alpha ,$$

where E_α is the alpha energy in GeV. Figure 3 shows this fit and experimental values of α at 0.6–3.3 GeV. For a target of thickness x_T (g/cm^2), the increase in apparent activity is therefore given by $\alpha[(x_T/2)+x]$, where x refers to the thickness of matter present in front of the target (telescope scintillator A). Although this technique does not take backward moving secondaries into account, the fact that the corrected results for 3, 6, and 10 mm targets show no systematic differences indicates that any such effect is small. These corrections for secondary production vary from a maximum of 4% at 0.64 GeV to 9% at 2.8 GeV, with a relative uncertainty of $\approx 10\%$ in the correction.

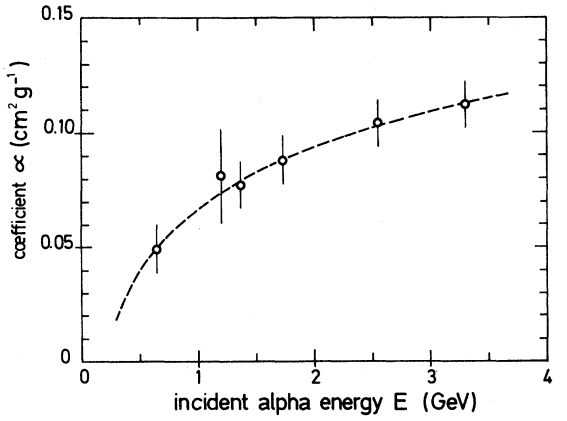

FIG. 3. Coefficient α of ^{11}C enhancement due to secondary particles created in the target. The points are experimental values (an average of several results). The curve is the least squares fit ($\alpha = 0.0665 + 0.0388 \ln E$).

IV. RESULTS

A total of 48 runs (12 at each energy) were accepted for the cross section fitting procedure described in the Appendix. During this analysis, certain measurement points were eliminated: one at 2.8 GeV and two at 0.64 GeV (the beam intensity

TABLE I. Measured cross section for the C(α,X)^{11}C reaction.

E_α (GeV)	No. of measure	Cross section (mb)	Random error (%)	Systematic error (%)
0.64	10	55.6±2.2	0.3	3.6
1.2	11	49.2±1.9	0.3	3.6
2.0	12	44.1±1.8	0.4	3.6
2.8	9	42.0±1.7	0.4	3.6

was too high), two at 2.8 GeV and one at 1.2 GeV (this was more than three standard deviations from the fit). The cross sections finally adopted, along with their errors, are given in Table I. The observed random error comes mainly from the counting statistics in determining the ^{11}C activity ($\approx 1\%$ from the decay fits). The systematic errors for each energy are 1.3% from the neutron beam contamination, 3% from ^{2}H contamination, 1% from the depth effect (secondary production), and 1% for the ^{11}C counting efficiency in the target, all of which combine quadratically to a total systematic error of 3.6%. The final error is the arithmetic sum of the random error and the systematic error.

Our results, and those available in the literature, are given in Fig. 4. The value obtained by Crandall *et al.*[12] at 380 MeV that is corrected in Ref. 2 (58.2±3) mb, that of Radin[4] at 920 MeV (48.9±1.8) mb, and our own values all show that the $C(\alpha,X)^{11}C$ reaction cross section decreases slowly from 380 MeV to 2.8 GeV, probably tending towards a constant value only beyond several GeV. Since these measurements were carried out, several other unpublished results have come to our attention; one at 700 MeV by Dollhopf[13] (50±4) mb, and two others,[14] one at 1.59 GeV (45.9±1.4) mb and one at 4.19 GeV (42.1±1.3) mb. These results are also given in Fig. 4. More details on this work, and related measurements with ^{2}H and ^{3}H projectiles, are given in Ref. 15.

Note added in proof. Reference 14 has since appeared as the following article, J. W. Geaga *et al.*, Nucl. Phys. A386, 589 (1982). Their final values are 46.4±1.3 mb at 1.59 GeV and 4.25±1.1 mb at 4.19 GeV, instead of 45.9 and 42.1, as quoted here.

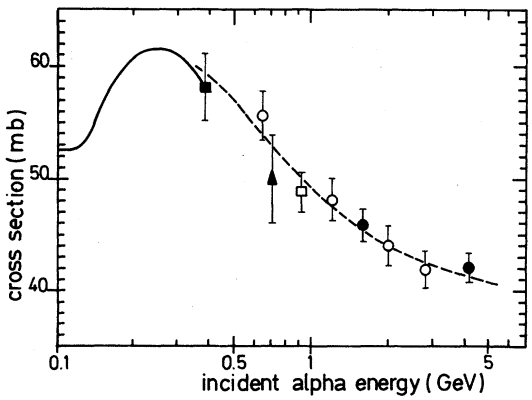

FIG. 4. Absolute cross section for the $(\alpha,X)^{11}C$ reaction. The symbols are as follows: □, Ref. 4; ■, Ref. 12, as corrected in Ref. 2; ▲, Ref. 13; ●, Ref. 14; ○, this work. The solid curve is from Ref. 2. The dashed curve is to guide the eye.

ACKNOWLEDGMENTS

We are very grateful to J. C. Brisson and J. Pascual for the loan of the telescope electronics and for their continual aid and advice. We thank J. Berger and L. Goldzahl for the loan of several electronic components and for their advice and discussions. We thank the staff of Saturne, especially M. Van den Bossche, for the fine beams given to us. One of the authors (J.R.R.) would like to thank the Centre National de la Recherche Scientifique for its support.

APPENDIX: CORRECTION FOR LOSSES DUE TO TELESCOPE DEAD TIME

A. Loss estimation by measurement of the random coincidence fraction

According to the type of dead time of the counting system,[16] the corrected cross sections have been calculated by the following expressions:

$$\sigma_a = \sigma(1-kR)^{-1} \tag{A1}$$

(nonextended dead time) or

$$\sigma_a = \sigma_j \exp(kR_j) \tag{A2}$$

(extended, also cumulative or paralyzable) with

$$R_j = R\exp(kR_{j-1})$$

and $R_1 = R$.

In these expressions we have the following: σ_a, the apparent cross section, obtained from the apparent flux S_{AB}; σ (or σ_j), the corrected cross section; k, the ratio of dead time τ of the direct coincidence line to resolution time θ_D (sum of pulse widths at the coincidence selector input) of the random coincidence line; and R, the ratio of total number of random coincidences S_D to the apparent flux S_{AB} recorded by the telescope at the end of irradiation.

Because a sufficient number of exposures were performed at each energy for a fairly wide range of intensities, it was possible to look for the best fit of expressions (A1) and (A2) to the experimental data R and σ_a, the coefficient k being considered a free parameter. This fit was made by the least squares method in an attempt to find the k value minimizing χ^2. Figure 5 shows at each energy (except 0.64 GeV, where the random coincidence circuit was not used) the fits adopted for expression (A1). The results given for these two expressions are very close (their difference is $<0.4\%$). It is worth noting that

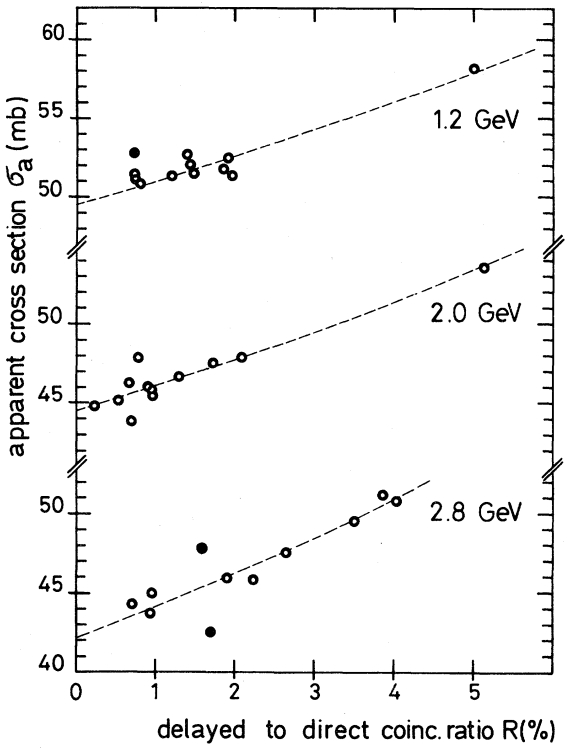

FIG. 5. Measured apparent cross section σ_a versus delayed to direct coincidence ratio R. The circles are experimental values (closed circles lying at more than three standard deviations from the fitted values have been eliminated). The best fits to the data using Eq. (A1) are indicated by the dashed curves.

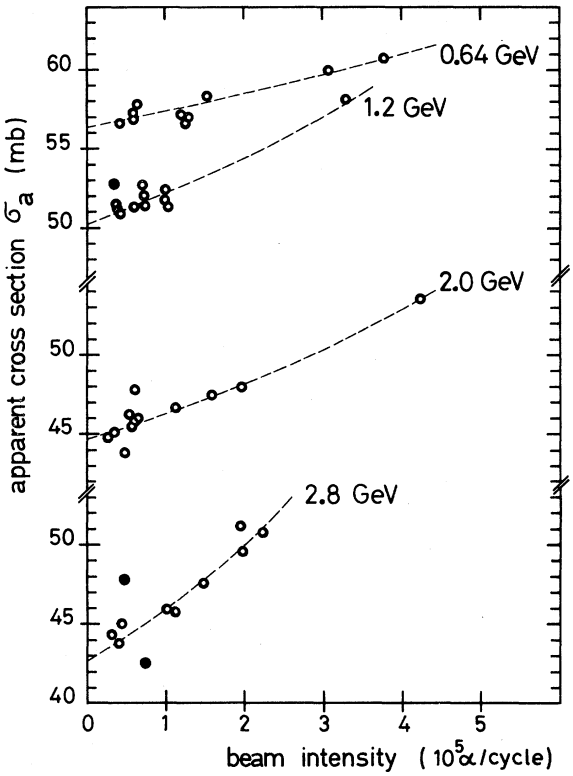

FIG. 6. Measured apparent cross section σ_a versus beam intensity (alphas per cycle); for symbols, see Fig. 5. The best fits to the data using Eq. (A4) are indicated by the dashed curves. The data of Figs. 5 and 6 are not corrected for neutron contamination (-1.3%).

the best values found for k ($\approx 3-4$) are considerably larger than the estimated ones ($k \approx 1.5-2$) on the basis of the off line measurements of θ_D and τ, with a double pulse generator ($\tau = 10$ ns, $\theta_D = 7.4$ ns), a random pulse generator ($\theta_D = 6.4$ ns), or by using a variable delay technique in the beam ($\tau = 14$ ns). The poor duty cycle of the α beam available for this experiment and the high particle fluxes utilized here are probably responsible for this difference (the effective duration of the beam spill, deduced from the random coincidence rate, has been found only between 35 and 60 ms, depending on energy).

B. Loss correction by extrapolation to zero intensity

The information delivered by the random coincidence circuit is ignored here. The correction for losses due to dead time is carried out by fitting a parametric expression, in which the independent variable is the mean intensity per cycle, to the experimental data. These expressions for the two kinds of dead time already considered are the following:

$$\sigma_a = \sigma[1-(\tau/\delta_e)(S_{AB}/p)]^{-1}\,, \tag{A3}$$

$$\sigma_a = \sigma_j \exp[-(\tau/\delta_e)(S_{AB}/p)_j]\,, \tag{A4}$$

with

$$(S_{AB}/p)_j = (S_{AB}/p)\exp[-(\tau/\delta_e)(S_{AB}/p)_{j-1}]\,,$$

where (S_{AB}/p) is the average intensity (particles per cycle) during exposure to a number of p cycles and δ_e is the "effective" duration of the beam spill [(τ/δ_e) is considered as a free parameter during the fitting procedure].

As seen in the preceding paragraph, the distinction between the two types of dead time is not very significant in our case. We only used expression (A4), and Fig. 6 shows fits which were found.

To conclude, the corrected cross sections obtained from Eqs. (A1), (A2), and (A4) are very close. The value finally adopted is the average of the two extreme values [Eqs. (A1) and (A4)] which is given in Table I (the difference mean value given by these two equations is $\approx 1\%$).

*Present address: Department of Geophysics and Planetary Sciences, Tel Aviv University, Ramat-Aviv, Israel.

[1]J. B. Cumming, Annu. Rev. Nucl. Sci. 13, 261 (1963).

[2]J. Tobailem, C. H. Lassus Saint-Genies, and L. Levêque, Commissariat à l'Energie Atomique, France, Saclay Report Nos. CEA-N 1466 (1), 1971 and CEA-N 1466 (3), 1975.

[3]S. B. Kaufman, M. W. Weisfield, B. D. Wilkins, D. Henderson, and E. P. Steinberg, Phys. Rev. C 13, 253 (1976).

[4]J. R. Radin, Phys. Rev. C 2, 793 (1970); 4, 1010(E) (1971).

[5]J. B. Cumming and R. Hoffman, Rev. Sci. Instrum. 29, 1104 (1958).

[6]P. J. Campion, Int. J. Appl. Radiat. Isotopes 4, 232 (1959).

[7]A. Gandy, Int. J. Appl. Radiat. Isotopes 11, 75 (1961); 13, 501 (1962).

[8]J. B. Cumming, C. Friedlander, and S. Katcoff, Phys. Rev. 125, 2078 (1962).

[9]A. M. Poskanzer, L. P. Remsberg, S. Katcoff, and J. B. Cumming, Phys. Rev. 133, B1507 (1964).

[10]G. W. Butler, S. B. Kaufman, E. P. Steinberg, and B. D. Wilkins, Phys. Rev. C 6, 1153 (1972).

[11]A. R. Smith and J. R. Radin, private communication.

[12]W. E. Crandall, G. P. Millburn, R. V. Pyle, and W. Birnaum, Phys. Rev. 101, 329 (1956).

[13]W. E. Dollhopf, thesis, College of William and Mary, 1975; quoted in W. E. Dollhopf *et al.*, Nucl. Phys. A316, 350 (1979).

[14]J. Carroll, private communication.

[15]H. Quéchon, thesis, Université de Paris XI–Orsay, No. 234, 1980.

[16]J. W. Müller, Nucl. Instrum. Methods 112, 47 (1973).